REPORT DOCUMENTATION PAGE

AFRL-SR-AR-TR-02-

0222

1. AGENCY USE ONLY (Leave blank)	2. REPORT DATE: 6/11/02	3. REPORT TYPE AND Final report; 1/1/00 to 12/31/00

4. TITLE AND SUBTITLE

Microstructure Effects on Creep Behavior of Next Generation of Refractory Alloys for Very High Temperature Applications

5. FUNDING NUMBERS

F49620-00-1-0080

6. AUTHOR(S)

Vijay K. Vasudevan and Keith J. Leonard

7. PERFORMING ORGANIZATION NAME(S) AND ADDRESS(ES)

University of Cincinnati,
Department of Materials Science and
Engineering, PO Box 210012, Room
501D ERC, Cincinnati, OH 45221-0012

8. PERFORMING ORGANIZATION REPORT NUMBER

Final

9. SPONSORING / MONITORING AGENCY NAME(S) AND ADDRESS(ES)

AFOSR/NA
Metallic Structural Materials, 801 North
Randolph Street
Arlington, VA 22203-1977
Program Monitor: Dr. Craig S. Hartley

10. SPONSORING / MONITORING AGENCY REPORT NUMBER

11. SUPPLEMENTARY NOTES

12a. DISTRIBUTION / AVAILABILITY STATEMENT

Public/Unclassified/Unlimited

20020719 140

13. ABSTRACT *(Maximum 200 Words)*

The primary objective of the present project was to gain a basic understanding of the effects of microstructure on the creep behavior of a new class of Mo-Si-B alloys that are being considered for very high temperature structural applications. A second objective was to obtain insight into the oxidation behavior of these materials. During this one-year project, thermal effects on microstructure evolution in a Mo-7.44Si-8.51B (at.%) alloy were studied. The results indicate that it is possible to exert some control over microstructure and properties by very high temperature heat treatments. Significant changes in volume fraction of α-Mo, Mo_3Si and T2 phases occur at temperatures ≥1700°C. The cyclic oxidation behavior in air at temperatures between 800-1100°C were also studied in a three-phase Mo-12Si-12B (at.%) and near-single T2 phase Mo-12.5Si-25B alloy: The results indicate that catastrophic oxidation occurs in both alloys at/below 800-900°C; performance and oxidation protection is better at ≥1000°C. A porous, non-protective borosilicate/B-SiO_2 layer forms at low temperatures, which permits easy oxygen diffusion and increased weight loss through volatilization of Mo as MoO_3 gas. A stable, dense silica scale forms at/above 1000°C, which provides protection from oxidation and reduced weight loss.

14. SUBJECT TERMS			15. NUMBER OF PAGES 28
			16. PRICE CODE
17. SECURITY CLASSIFICATION OF REPORT Unclassified	18. SECURITY CLASSIFICATION OF THIS PAGE Unclassified	19. SECURITY CLASSIFICATION OF ABSTRACT Unclassified	20. LIMITATION OF ABSTRACT None

MICROSTRUCTURE EFFECTS ON CREEP BEHAVIOR OF NEXT GENERATION OF REFRACTORY ALLOYS FOR VERY HIGH TEMPERATURE APPLICATIONS

Final Report

Work Performed Under

Grant No.: F49620-00-1-0080

Period: 1/1/00 to 12/31/00

Submitted By

Vijay K. Vasudevan, Principal Investigator
and Keith J. Leonard

Department of Materials Science and Engineering, University of Cincinnati
Cincinnati, OH 45221-0012

To
Dr. Craig S. Hartley
Air Force Office of Scientific Research/NA
Metallic Structural Materials, 801 North Randolph Street
Arlington, VA 22203-1977

June 13, 2002

TABLE OF CONTENTS

1. Research Objectives

The primary objective of the present project is to gain a basic understanding of the effects of microstructure on the creep behavior of a new class of Mo-Si-B alloys that are being considered for very high temperature structural applications. A second objective is to obtain insight into the oxidation behavior of these materials

2. Introduction

A recent discovery of the possibility for enhanced oxidation resistance [1,2] have led to the identification of a revolutionary class of ductile matrix-brittle intermetallic phase alloys based on the Mo-Si-B system as promising candidates for structural applications at very high temperatures (1000-1600°C), and are beginning to lead to intensive research into the oxidation behavior [3-6], microstructure [7] and mechanical properties [8] of these materials. The overall aim of this project, which was closely coupled with ongoing research activities at the Air Force Research Laboratory (AFRL), was to address three issues related to the creep behavior of these materials: 1) basic materials and microstructural studies; 2) evaluation of the creep phenomenology and establishment of the constitutive behavior of these materials; and 3) theoretical modeling of the creep behavior based on analysis of the associated creep data, creep mechanisms, damage processes and microstructural parameters. A secondary goal was to evaluate and understand the oxidation behavior of these materials.

3. Status of Effort

During the one-year of this project, effort was directed toward basic materials and microstructural studies and the oxidation behavior. Materials for these studies were obtained from Dr. Madan Mendiratta of UES/AFRL, Dayton, OH, and the present effort was closely coupled with ongoing research activities there. The effects of heat treatment on microstructure evolution in a Mo-7.44Si-8.51B (in at.%) alloy was studied and the microstrcutures characterized

by electron-optical methods, XRD and hardness measurements. In addition, the cyclic oxidation behavior, together with accompanying changes in microstructure, was also studied. The results obtained are presented and discussed in detail in the following section.

4. ACCOMPLISHMENTS

4.1. Effects of Heat Treatment on Microstructural Evolution

The aim of this part of the work was to (a) develop a solid understanding of the microstructure of the selected Mo-Si-B alloy, (b) evaluate the effects of thermal influences on microstructure stability, and (c) establish conditions necessary for producing controlled microstructures for testing. This work was performed by a postdoctoral research associate, Dr. Keith J. Leonard.

Experimental Details

Cut samples of an Mo-7.44Si-8.51B (in at.%) (Mo-2.5Si-1.4B in wt.%) alloy that had been sectioned from a cast and then 1800°C-extruded ingot, were obtained. This alloy was expected to have a three-phase microstructure consisting of α-Mo, Mo_3Si and Mo_5SiB_2 (T2) phases, based on the current ternary phase diagram [7]. Microstructural changes were evaluated through 50h vacuum furnace heat treatments of the as-extruded material at a range of temperatures (1000-1900°C). Single-step and two-step heat treatments were performed. The microstructures were examined by back-scattered electron (BSE) imaging in an SEM, and phase fractions measured by quantitative image analysis. Phase identification was achieved through x-ray diffraction (XRD). Hardness measurements were made on both the macroscopic scale using a Rockwell C indentor under 150 kg load held for 30s, and on the microscopic scale using a Vickers diamond indentor under 1 kg load held for 20s. Microhardness measurements were also made on the α-Mo ohase in selected samples using a reduced load of 100g.

Results and Discussion

The results of the effects of heat treatment on the phase fractions and hardness are given in Table 1 and representative microstructures, XRD traces and plots of hardness and phase fractions as a function of heat treatment are displayed in Figures 1-3, respectively.

The as-extruded material had a microstructure of elongated α-Mo grains with pockets of the intermetallic phases in between (Figure 1(a)). The α grains were not totally uniform, and regions containing large pockets of α (primary dendrites in the cast ingot) that had not been sufficiently broken down during extrusion, were present. The intermetallic regions contained Mo_3Si and T2-Mo_5SiB_2 phases as detected by XRD (Figure 2). Careful examination was required to discriminate between the Mo_3Si and T2 phases in BSE images, due to the similarity of contrast. The as-extruded material contained the highest amount of the α -Mo phase, nearly 70%, coinciding with the lowest hardness value relative to all the heat-treated materials examined (Table 1, Figure 3(b)).

Heat treatments of the as-extruded material at lower temperatures (1000-1400°C), Figure 1(b,c), did not lead to an appreciable change in the morphology of the α grains. An increase in the volume fraction of Mo_3Si was measurable through XRD (Figure 2(b)) and BSEI (Figure 3(a), Table 1), with a corresponding increase in the hardness (Table 1, Figure 3(b)). The combined volume of both intermetallic phases was greater than that in the as-extruded material; this increase appeared to have occurred through the formation of coarse intermetallic particles around pre-existing particles, rather than by precipitation within α. The slightly higher macro- and micro-scale hardness of the 1200°C sample, however, suggests that some precipitation may have occurred within the α -Mo, which, though generally too fine to be discernible by BSEI, could also be seen occasionally (Figs. 1(b,c). An increase in the amount of the T2 phase was noted after heat treatment. Furthermore, formation of α-Mo grains within clusters of intermetallic articles was also seen (Figures 1(b,c)).

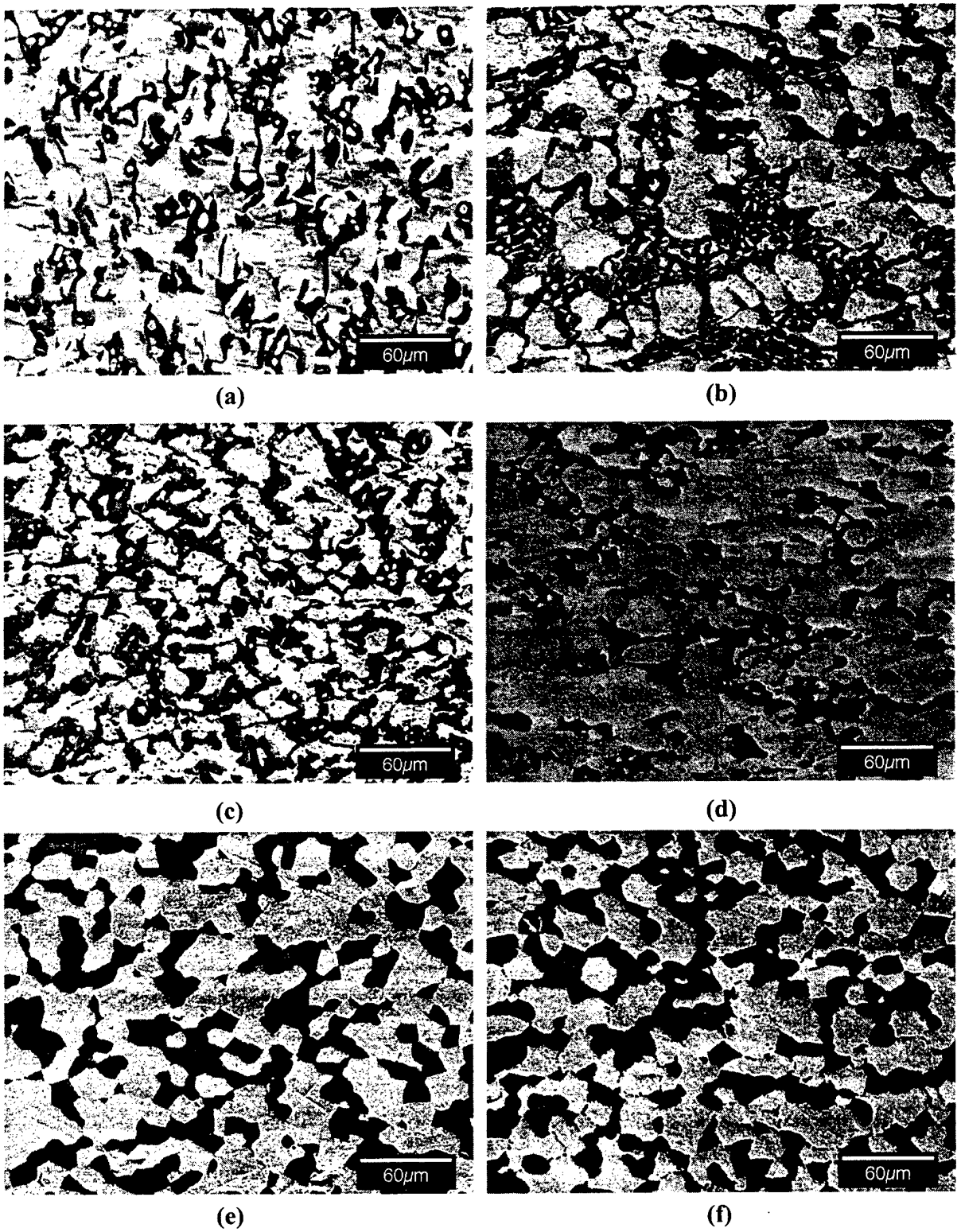

Figure 1. BSE micrographs showing microstructure of the Mo-7.44Si-8.51B alloy. (a) As-extruded (AE) at 1800°C; (b) AE + 1200°C, 50h; (c) AE + 1400°C, 50h; (d) AE + 1700°C, 50h; (e) AE + 1900°C, 50h + 1200°C, 50h; and (f) AE + 1900°C, 50h + 1400°C, 50h. Light–α-Mo, dark/gray–intermetallic.

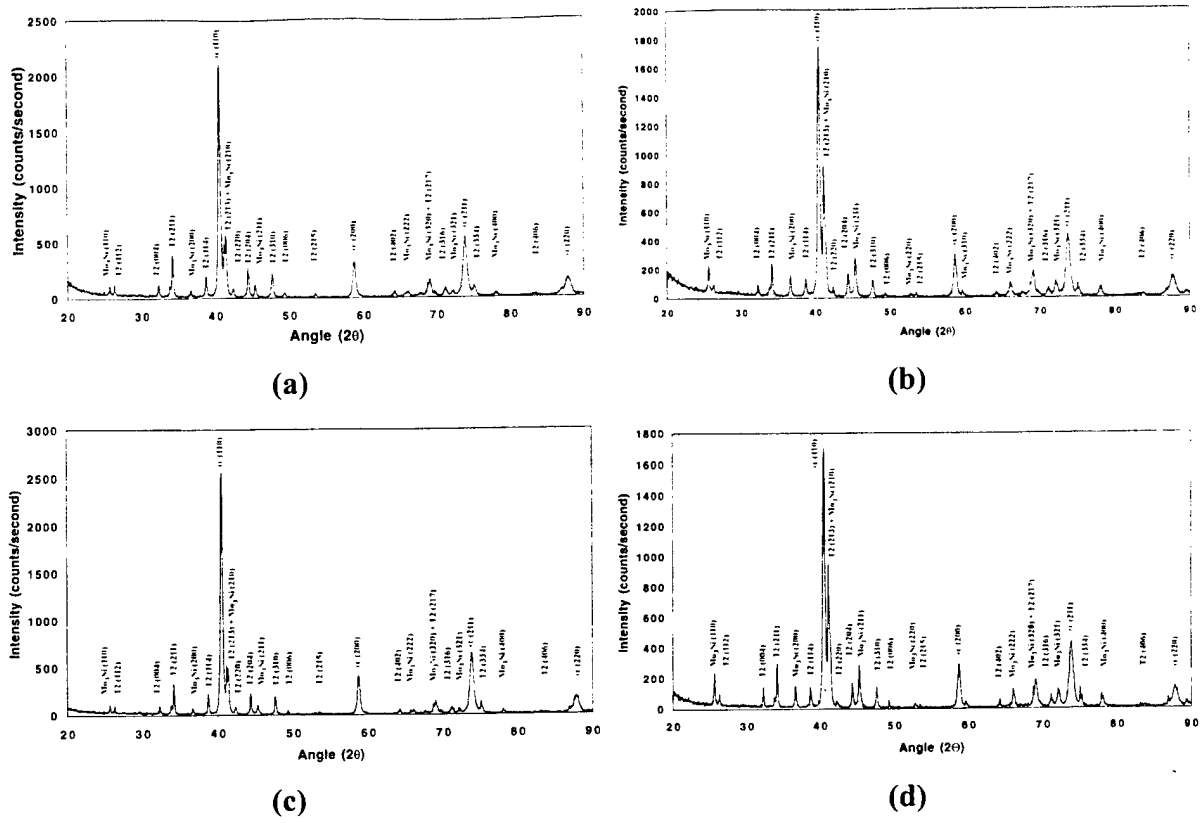

Figure 2. Representative XRD traces of the Mo-7.44Si-8.51B alloy. (a) As-extruded (AE) + 1200°C, 50h; (c) AE + 1700°C, 50h; and (d) AE + 1900°C, 50h + 1400°C, 50h.

TABLE 1

Hardness and Phase Fractions as a Function of Heat Treatment of the Mo-7.44Si-8.51B Alloy

Treatment	Rockwell C (kg/mm^2)	Microhardness HV (kg/mm^2)	Microhardness α -only	%T2	$\%Mo_3Si$	% alpha-Mo	% Intermetallic
As-Extruded	48.48	496.4				70.91	29.09
Ext+1600/1700/1500C	48.43			14.72	35.29	49.99	50.01
Ext+1000C	49.2	563.3				63.4	36.6
Ext+1700C	49.4	512	460.9	14.7	18.19	67.11	32.89
Ext+1900/1400C	49.82	600.4	529.1	23.5	26.31	52.19	49.81
Ext+1400C	50.12	554.8		12.6	33.3	54.1	45.9
Ext+1200C	50.84	647.84		11.21	33.72	55.07	44.93
Ext+1900C	52.2	651	546.9	21.32	21.95	56.73	43.27
Ext+1900/1200C	54.21	655.1	567.7	14.51	26.86	58.63	41.37

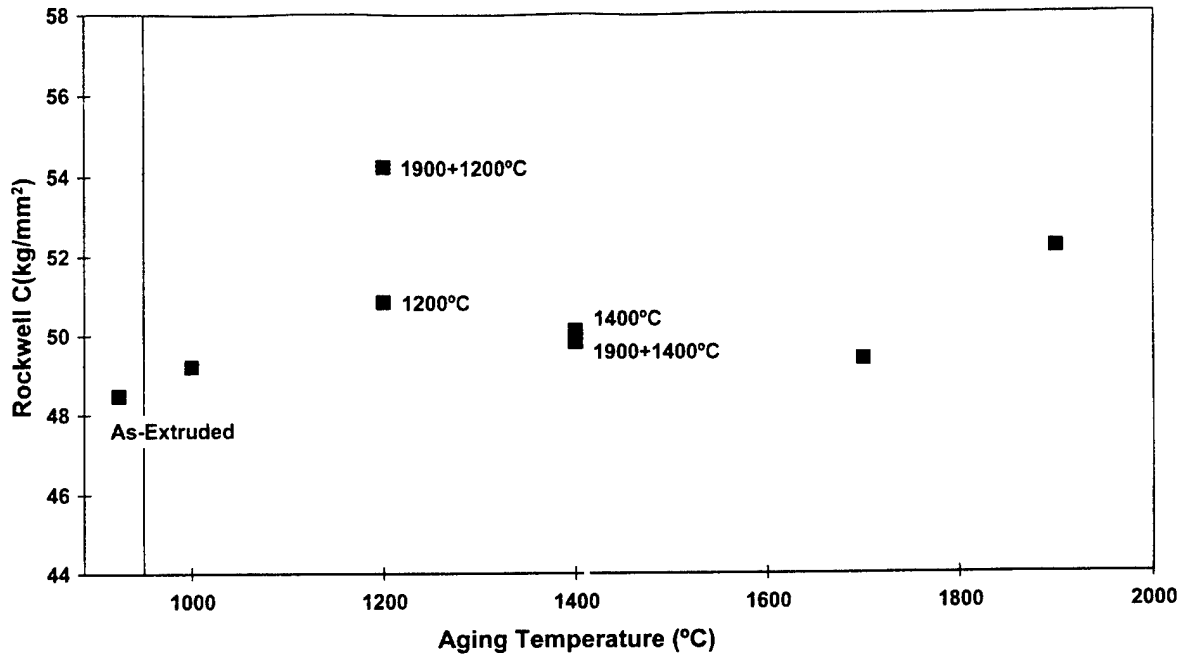

(a)

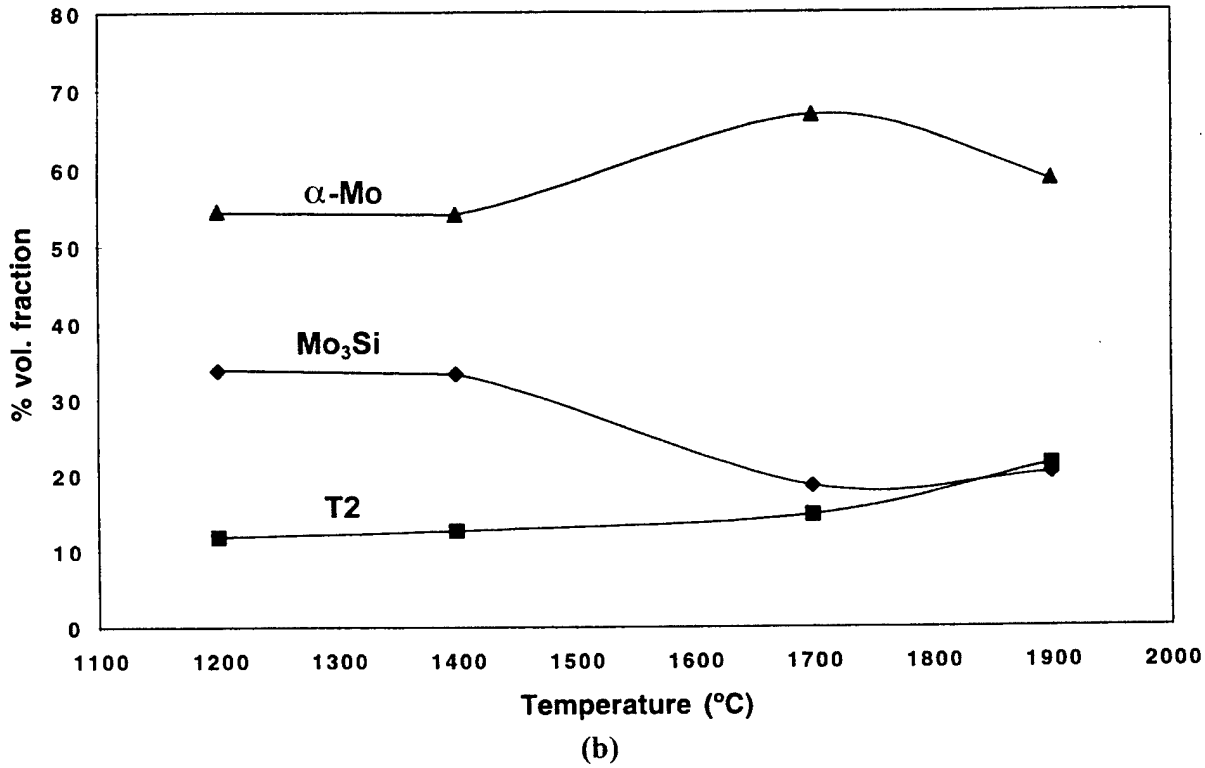

(b)

Figure 3. (a) Volume fractions of phases and (b) hardness as a function of heat treatment of the Mo-7.44Si-8.51B alloy.

A large change in microstructure (Figure 1(d)) and hardness (Table 1, Figure 3(b)) was observed in the 1700°C material compared with the aforementioned samples. XRD patterns, Figure 2(c), revealed stronger T2 peak intensities relative to Mo_3Si compared with those observed in samples heat treated at lower temperatures. Although an increase in the amount of T2 was apparent, the overall peak intensities of the intermetallic phases were decreased relative to those of the α phase. The measured α volume fraction (Figure 3(a)) was comparable to that in the as-extruded material, supporting the XRD results. The substantial increase in the volume fraction of the α phase (Figure 3(a), Table 1) was reflected in the decrease in hardness, which was again comparable to the as-extruded and 1000°C-heat treated materials.

Samples heat treated at 1900°C, Figure 1(e,f), however, showed a large decrease in the amount of α-Mo and a substantial increase in the amount of T2 (Figures 2(d), 3 and Table 1) compared with the 1700°C heat-treated sample, while the amount of Mo_3Si remained relatively unchanged. The changes in phase fractions, which also correlate with hardness changes, indicates a possible change in phase equilbria between 1700 and 1900°C. Additional samples were heat treated at 1700 and 1900°C, and it was confirmed that the changes observed were not an effect due to inhomogeneity of the starting materials. Microhardness measurements using a reduced load, indicated that the α-Mo was ~16% harder in the 1900°C heat-treated materials than that in the 1700°C heat-treated samples. Whether fine-scale precipitation of intermetallic phases within the α-Mo had occurred during cooling remains to be ascertained.

Heat treatment of the 1900°C material at 1400°C for 50h produced a microstructure that exhibited the most uniform distribution of the three phases (Figure 1(f)). Although the volume fraction of T2 remained relatively unchanged and the amount of Mo_3Si increased relative to the 1900°C material, the microhardness decreased significantly. This is believed to be due to the homogeneous microstructure and distribution of phases. The oxidation behavior and mechanical properties of samples subjected to this heat treatment would be of interest.

The microstructure of the 1900°C+1200°C material (Figure 1(e)) contained a higher amount of α than that in the 1900°C+1400°C material, but comparable to that of the 1900°C

material. However, there was a reduction in the amount of T2 with a corresponding increase in the amount of Mo_3Si over the 1900°C material as seen in the single-step heat treatments between 1200 and 1900°C (Table 1). Although the α volume fraction was negligibly reduced in the 1900°C+1200°C treatment in comparison with the 1900°C condition, the T2 and Mo_3Si amount changed significantly. Counter to the previously observed dependence of microhardness on volume fraction of α, the 1900°C+1200°C material exhibited the highest hardness amongst all samples studied. Because of the high amount of α remaining in the microstructure after cooling from 1900°C to 1200°C, it is possible that fine-scale precipitation of intermetallics has occurred within the α phase. This in part is further supported by the large change in microhardness of the α phase. In the 1900°C+1400°C material, which displays a lower hardness, the 200°C higher temperature relative to the 1200°C material and, hence higher diffusivity, may have allowed new intermetallic particles to form at/around preexisting particles rather than within the α -Mo grains.

Close examination of the microhardness indentations revealed that cracks formed on the intermetallic particles were deflected by the α-Mo grains, which points to a potential toughening effect of the latter. Previous studies [7] have suggested that diffusivity in the Mo-Si-B system is extremely low and that microstructural changes are difficult to bring about by heat treatment at temperatures below 1600°C. The present results indicate, however, that by utilizing very high heat treatment temperatures (≥1700°C), it is possible to effect significant changes in microstructure and hardness of these materials and that it will be possible to exercise control over both using such methodologies.

4.2. Cyclic Oxidation Behavior

The aim of this part of the work was to evaluate the oxidation behavior and elucidate oxidation mechanisms of these materials. This work was performed by a UG student, Brian Kowalski, as part of his senior project, and by postdoctoral research associate Keith Leonard.

Experimental Details

For this study, two Mo-Si-B alloys, Mo-12Si-12B and Mo-12.5Si-25B (in at.%), referred to as Mo1212 and Mo1225, respectively, were obtained as arc-cast buttons. The Mo1212 alloy was homogenized by HIPping at 1500°C, 107MPa for 6h and successive heat treatments at 1600, 1700 and 1500°C for 24h each, to produce a homogeneous three-phase microstructure of α-Mo , Mo_3Si and T2. The cast Mo1225 sample was homogenized at 1700°C for 24h.

Test samples of 6 mm x 6 mm x 10 mm of the homogenized alloys were electro-discharge machined (EDM) for cyclic oxidation tests. Prior to testing, the oxide scale produced during EDM cutting was removed from each side with 800 grit polishing paper. Cyclic oxidation tests were performed in air at temperatures of 800, 900, 1000 and 1100°C, by placing the test samples in Al_2O_3 boats within a carefully monitored box furnace. Oxidation exposure times between measurements of weight loss were staggered between the minimum and maximum times of 15 minutes to 388 hours, with the majority of the measurements taken at short intervals near the beginning of the oxidation tests.

Characterization of the oxide scale (surface and cross-section) was performed on a Hitachi S-4000 field-emission scanning electron microscope (SEM) fitted with a Link EDS system. X-ray diffraction of the oxide scale products, which were found to be adherent to the sample surfaces, was conducted in a computer-automated Philips PW1729 diffractometer.

Results

The cast microstructure of the Mo1225 material, Figure 4(a), contained long plates of the T2 phase formed through the decomposition of a higher temperature phase that had solidified from the melt. This microstructure correlates with the possible MoB primary solidification field from which the composition of the T2 based alloy falls into, as determined by Nunes *et al.* [7]. In the cast microstructure, the regions between the T2 plates contained a mixture of α-Mo solid solution, Mo_3Si and T2, as verified by XRD (Figure 5(a)). Following homogenization of this alloy at 1700°C, 24 h, the T2 laths could still be distinguished, though the α and Mo_3Si volume fractions were significantly reduced along with an increase in width of the T2 laths (Figure 4(b)).

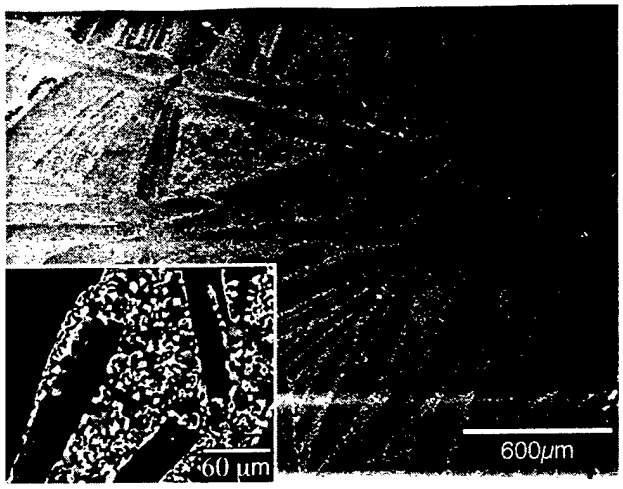

(a)

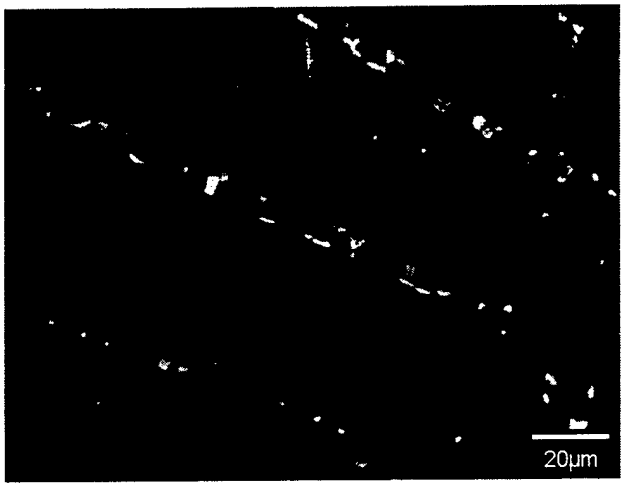

(b)

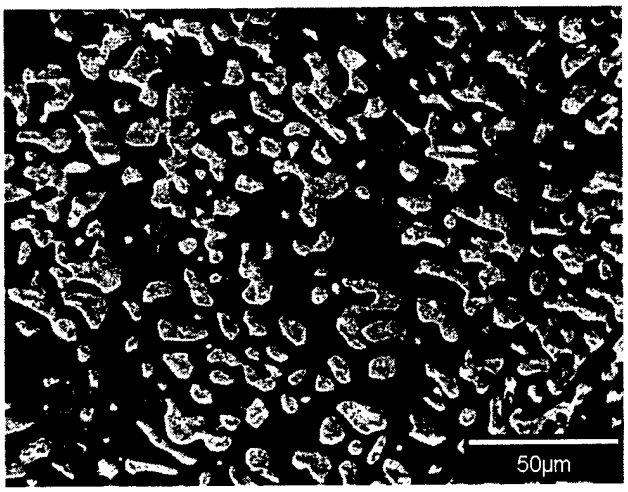

(c)

Figure 4. BSE micrographs showing microstructure of (a) As-cast Mo-12.5Si-25B alloy, (b) as-cast+ homogenized (1700°C, 24h) Mo-12.5Si-25B alloys and (c) as-cast + homogenized Mo-12Si-12B alloy.

The microstructure of the homogenized Mo1212 material (Figure 4(c)) contained a random distribution T2 and Mo_3Si particles in a matrix of α (Figure 5(b)). The α grains were discontinuous throughout the samples, although a bimodal size distribution was observed. This distribution is believed to be the result of a significant increase in the volume fraction of α at 1700°C [current work], rather than from the removal of the segregation from solidification.

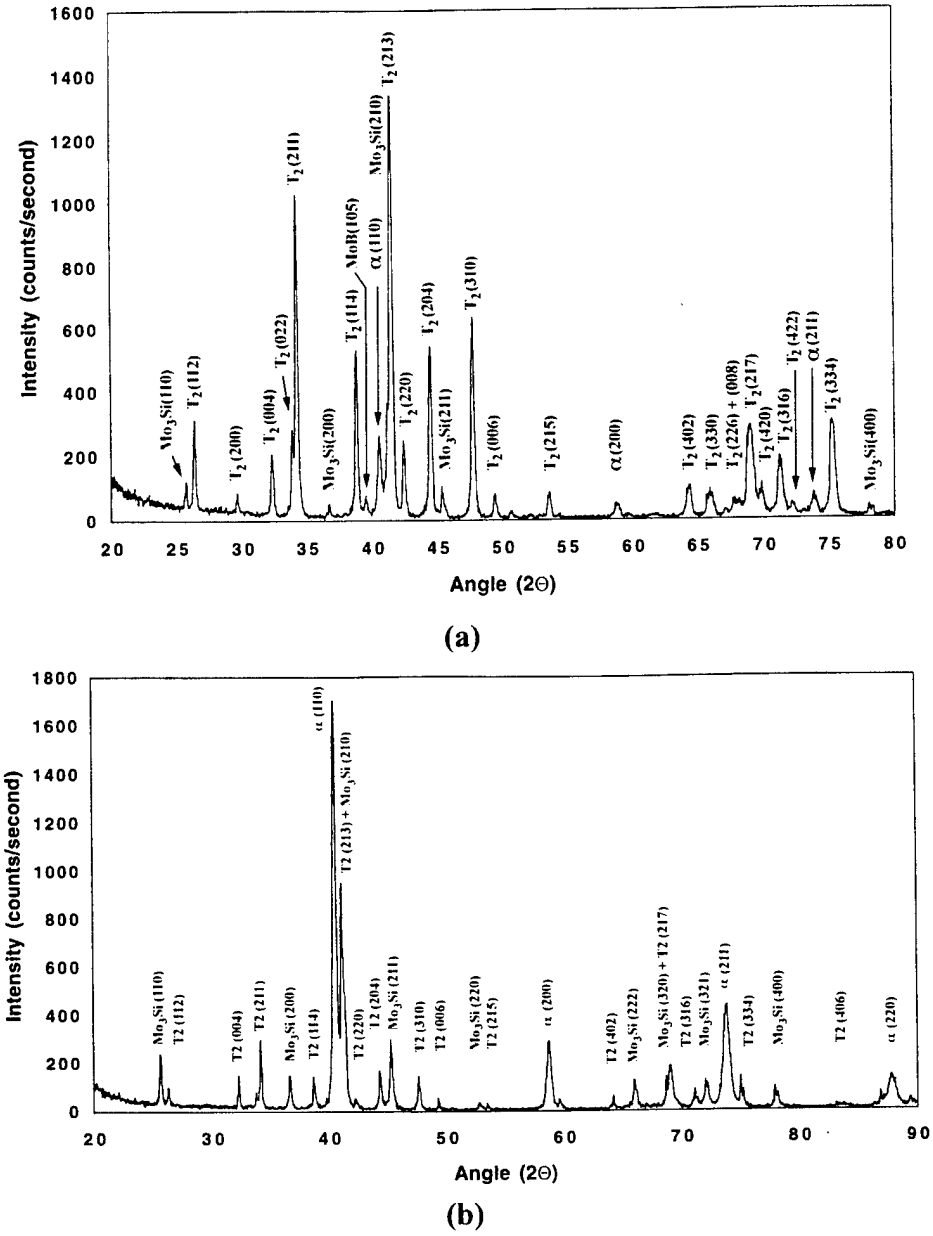

Figure 5. XRD traces of (a) as-cast Mo-12.5Si-25B T2 alloy and (b) homogenized (HIPped 1500°C, 107Mpa, 6h + 1600°C,24h+ 1700°C.24h + 1500°C,24h) Mo-12Si-12B alloy.

The cyclic oxidation behavior of Mo1212 was investigated at 900, 1000 and 1100°C and the results are displayed as wt. loss/initial surface area vs. time in Figure 6. As can be seen, following the initial transient, the wt. loss levels off to a low and near-constant value on exposure at 1000 and 1100°C, with the total wt. loss being lower in the latter. On the other hand, exposure at 900°C led to rapid wt. loss after about 4h. Due to catastrophic failure of the sample after only 4h at this temperature, lower temperature cyclic oxidation tests were not conducted, but have been reported by others [9]. The weight loss which occurred within the first few minutes was slightly greater in the 1000°C sample than in the 900°C material, which were both much greater than that observed in the 1100°C exposed material. Extrapolation of the curves backwards in time to the origin is not possible due to an initial weight gain from oxygen absorption upon exposure [3,4] and the inherent temperature versus time lag of the sample during heating to the test temperature.

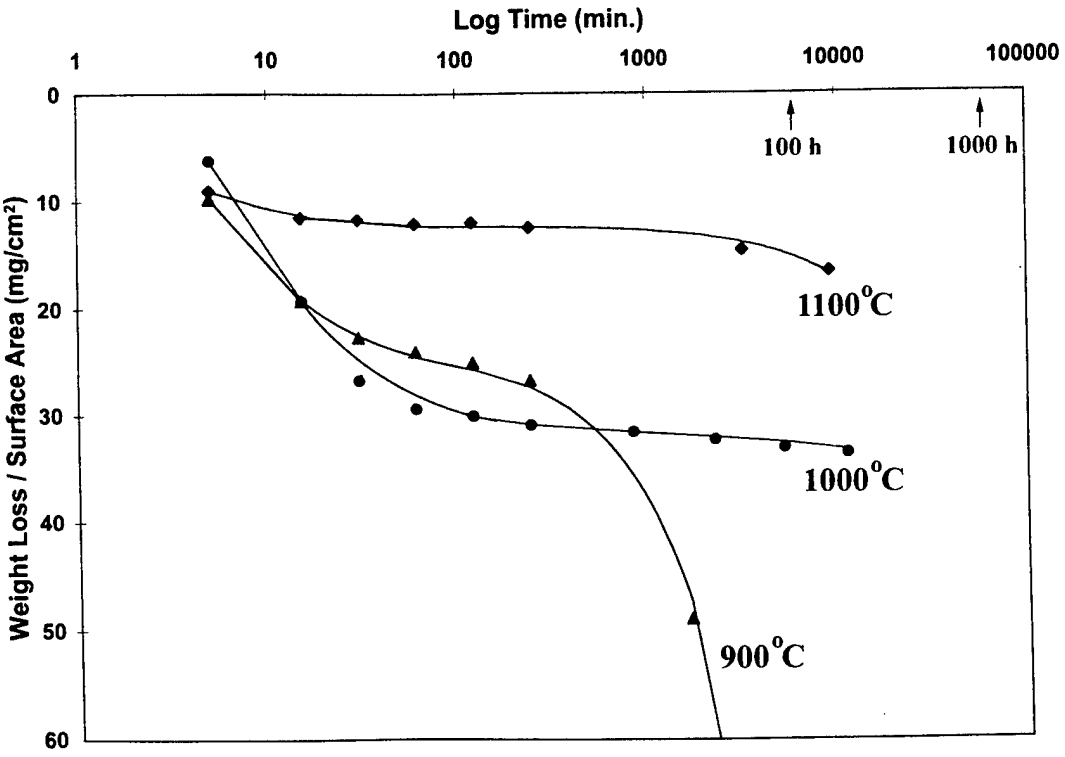

Figure 6. Wt. Loss/initial surface area vs. exposure time during cyclic oxidation in air of the homogenized, three-phase Mo-12Si-12B alloy.

Micrographs of the surface and cross-sections of the oxide scale produced at increasing times for the Mo1212 alloy at 900 and 1000°C are presented in Figures 7 and 8, respectively. It was observed that a glass-like boro-silicate scale was immediately produced over the surface of the sample, which when viewed under back-scattered electron imaging also revealed cavities and particles embedded in the glass (Figure 7(a)). These particles could not be clearly identified in cross-section, although it was observed that the thickness of the glass scale was greatest in the regions where the intermetallic Mo_3Si and T2-Mo_5SiB_2 grains of the base metal were in contact with the glassy material (Figures 7(b), 8(b)). The rapid formation of the boro-silicate glass at the expense of the Mo_3Si and T2 phases would produce an excess of Mo, which is presumed to have oxidized and formed the spherical particles within the scale. The formation of the scale was similar at short times in both the 900 and 1000°C-exposed materials.

Further exposure of the Mo1212 alloy at 900°C led to thickening of the glassy layer to a maximum of ~400 μm at the end of the test cycle of 178 hours (Figure 7(e)). It was observed both by examination of the surface and cross-section that the boro-silicate layer was porous, and contained Mo oxide particles and bubbles within it. These bubbles could be seen clearly after 4h through SEM observations of the surface (Figure 7(c)) and cross-section (Figure 7(d), prior to the over growth of the Mo oxidation products. Thus, the glassy scale seemed to be less viscous and more permeable to oxygen at this temperature.

The oxide scale products were also analyzed by XRD of the untampered surfaces of the exposed samples. It was determined that at short times at 900 and 1000°C, Figures 9(a) and 10(a) respectively, both MoO_3 and MoO_2 were present within the scale. In addition B_2O_3 peaks were also detected. The substantial loss of weight that occurred at 900 and 1000°C relative to that at 1100°C, is a result of the oxide products formed within this temperature range. At the lower temperatures, Mo oxidizes more readily into MoO_2 and MoO_3 whereas at higher temperatures a passivating SiO_2 layer is formed [3-6]. The higher initial weight loss observed at 1000°C relative to 900°C, is believed to be due to an increase in the initial oxidation rates with temperature.

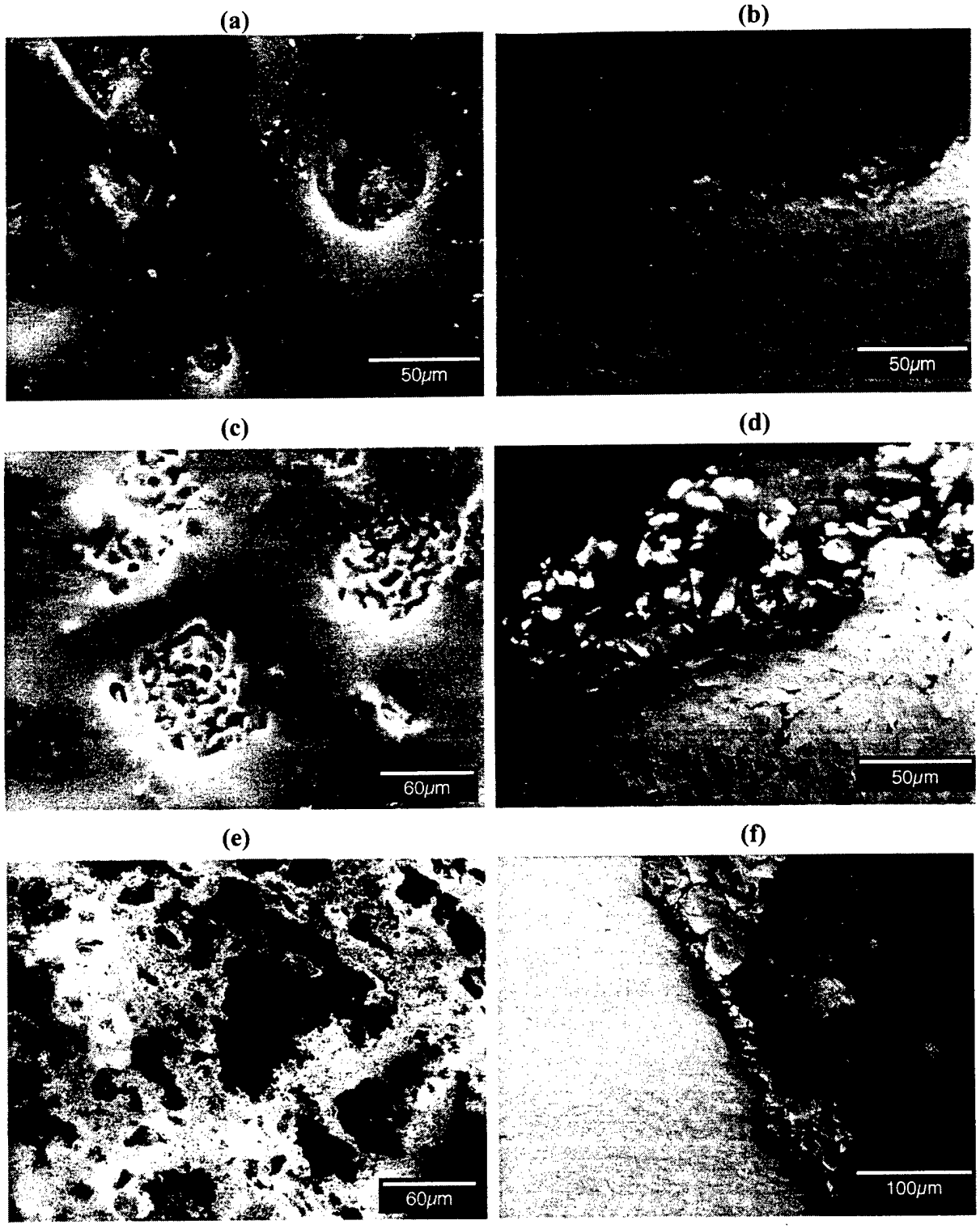

Figure 7. Microstructure of the oxide scale in the Mo-12Si-12B alloy exposed to air at 900°C for various times. (a) 15 mins, surface, SEI; (b) 15 mins., cross section, BEI; (c) 4h, surface, SEI; (d) 4h., cross section, BEI; (e) 15h, surface, BEI; (f) 15h, cross section, BEI; (g) 178h, surface, SEI; (h) 178h, cross section, BEI.

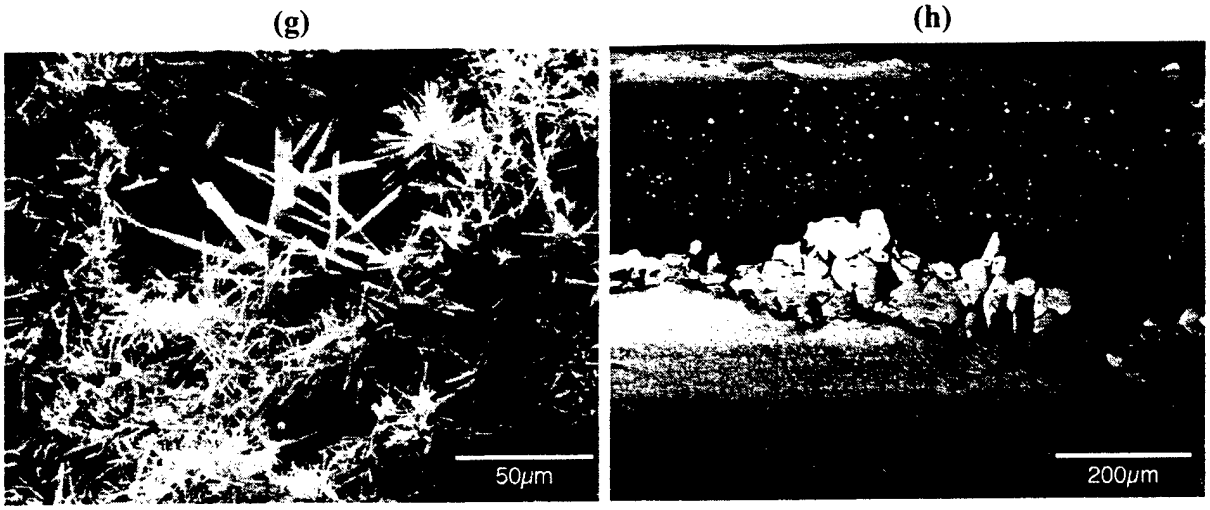

Figure 7. Continued.

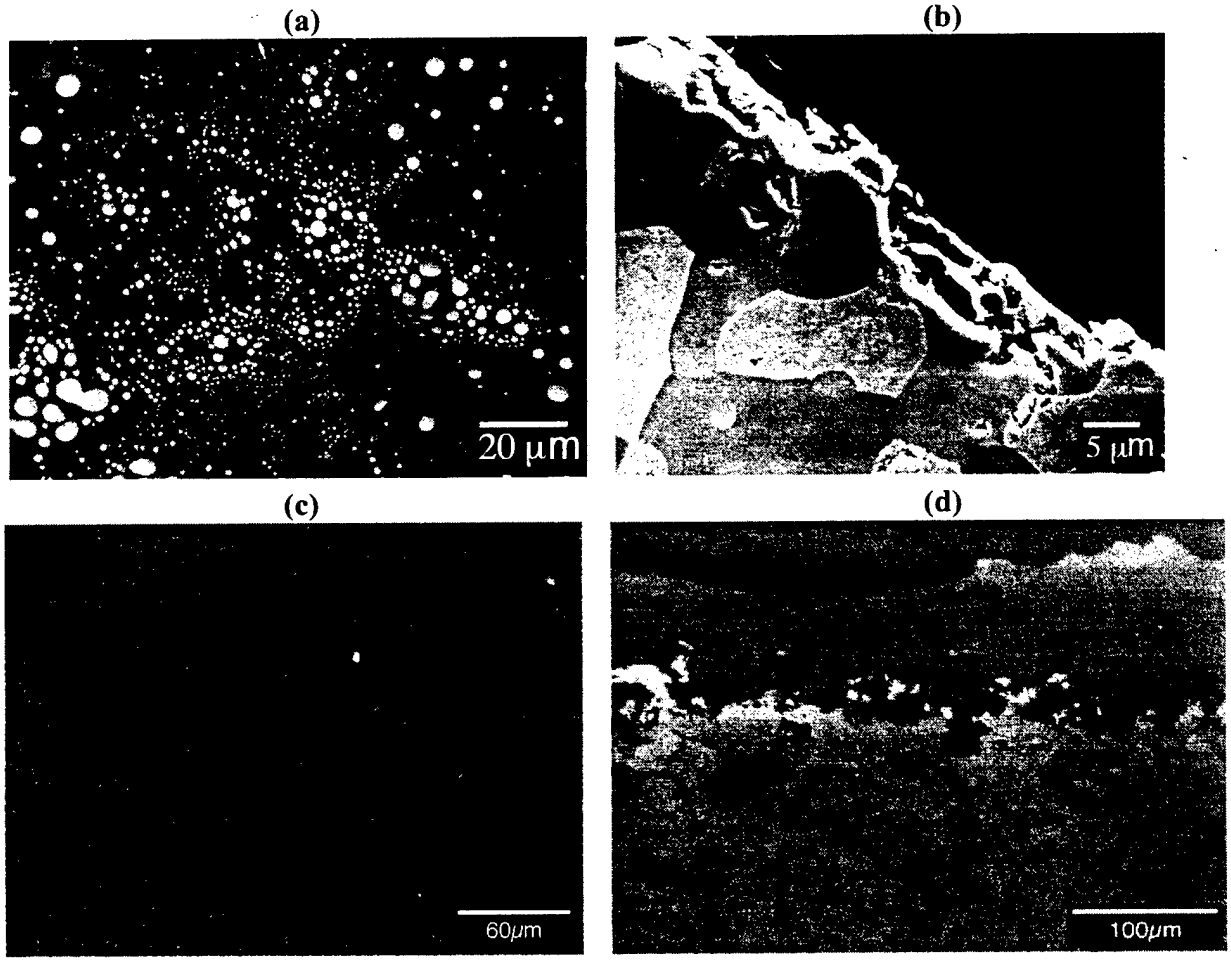

Figure 8. Microstructure of the oxide scale in the Mo-12Si-12B alloy exposed to air at 1000°C for various times. (a) 15 mins, surface, BEI; (b) 15 mins., cross section, BEI; (c) 188h, surface, BEI; (h) 188h, cross section, BEI.

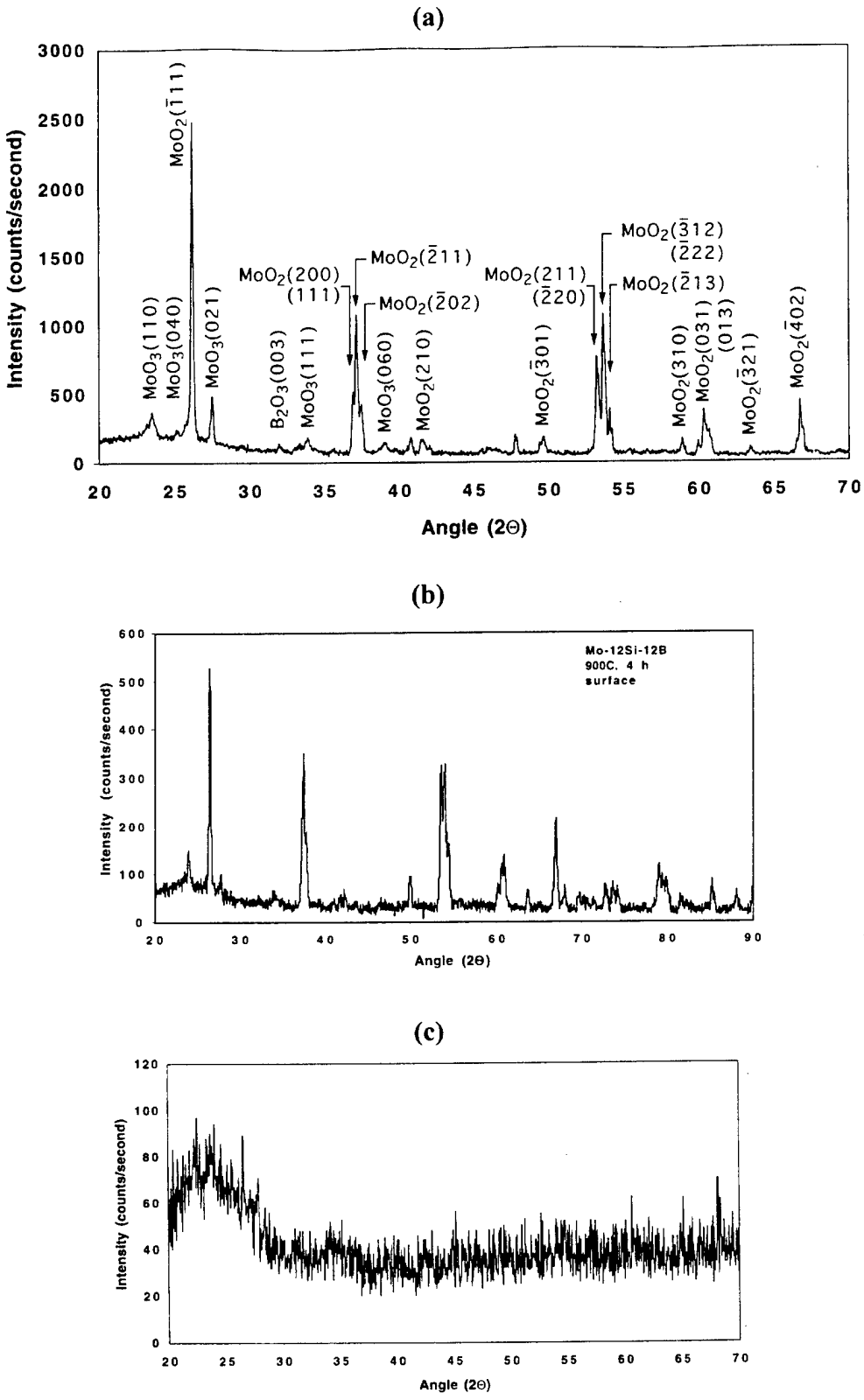

Figure 9. XRD patterns recorded from the surface of the oxide scale in the Mo-12Si-12B alloy exposed to air at 900°C for (a) 15 mins (b) 4h and (c) 178h.

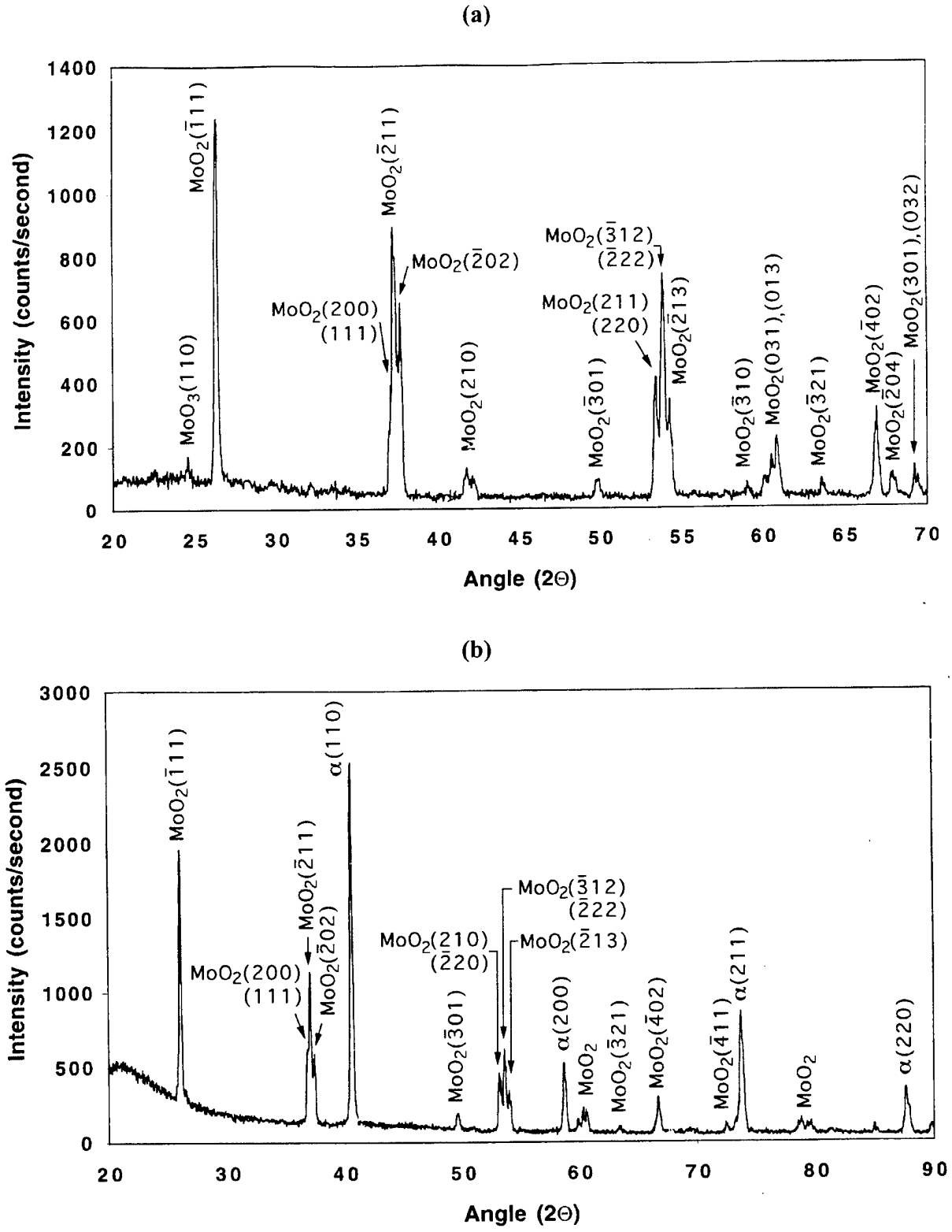

Figure 10. XRD patterns recorded from the surface of the oxide scale in the Mo-12Si-12B alloy exposed to air at 1000°C for (a) 15 mins and (b) 188h.

The compositions of oxide particles in the polished cross-sectioned samples were determined through EDS, and confirmed to be a mixture of MoO_3 and MoO_2 in addition to off stoichiometric compositions. The MoO_3 and MoO_2 particles appeared morphologically similar and could only be identified through composition analysis.

The catastrophic failure of the 900°C tested sample after 4h, could be seen through the cross-sectional SEM images (Figure 7(b,c)) as the persistent growth of the glassy scale on the sample surfaces. The porous scale permitted easy oxygen diffusion to the base metal and subjected the reaction surface to a higher oxygen partial pressure [3-6], thereby contributing to rapid oxidation. The increased oxygen content within the surface is believed to have allowed the formation of MoO_3 from the MoO_2, which being more volatile than MoO_2, escaped to the surface of the scale causing the increased rate of oxidation at 900°C. The presence of MoO_3 in the scale at 4h was confirmed through XRD (Figure 9(b)), which showed an increase in the intensity of peaks of the MoO_3 phase relative to MoO_2 in comparison with those after the 15-minute exposure (Figure 9(a)). XRD analysis of the surface after 4h revealed an amorphous structure with no detectable crystalline phases (Figure 9(c)), since the glass scale now exceeded a thickness of 200 μm.

The glass scale formed at 1000°C was much more protective than that in the 900°C material, and did not contain any evidence of a porous structure. At short times, spherical particles of MoO_2 and MoO_3 could be seen embedded in the glassy scale (Figure 8(a)) and evidence for these two oxides was seen in the corresponding XRD pattern (Figure 10(a)). At longer times, the sample surface was covered more or less completely by a stable, adherent glassy silica scale (Figures 10(c,d)). While XRD analysis of the 1000°C tested material after 188 h still showed the presence of MoO_2 (Figure 10(b)), the MoO_3 phase was not detected, indicating that the scale, which is now silica, was more resistant to oxygen diffusion, thereby causing a lower oxygen partial pressure and slowing the reaction kinetics. While the formation of a more stable protective scale above 900°C could not be characterized through XRD, its effect could be

seen by the increase in α-Mo solid solution at the metal/scale interface and the predominance of the α(110) peak in the XRD pattern.

The lowest oxidation rate of the Mo1212 sample occurred at 1100°C. The surface and cross-section of the sample after 154 h showed the formation of a smooth, uniform, pore-free scale with a thickness less than 60 μm. At this temperature, the formation of the protective silica scale was fast enough to have prevented the excessive weight loss due to MoO_3 volatilization as observed at 1000°C (Figure 6).

The Mo1225 T2 sample did fare better than the Mo1212 sample at 900°C (Figure 11). However, the sample did show similar catastrophic failure after 4h at 800°C as the Mo1212 sample at 900°C. The surface morphology of the Mo1225 sample after exposure at 800°C for 15h (Figure 12(a)) appeared with a flake-like oxide covering the surface. The glassy surface itself showed substantial cracking, suggesting a lower viscosity of the glass at 800°C inhibiting its ability to heal from repeated thermal cycling. The plate-like oxide particles are significantly different from the more needle-like particles observed in the Mo1212 sample (Figure 7(g)). The composition and structure of the flake-like particles have not been determined.

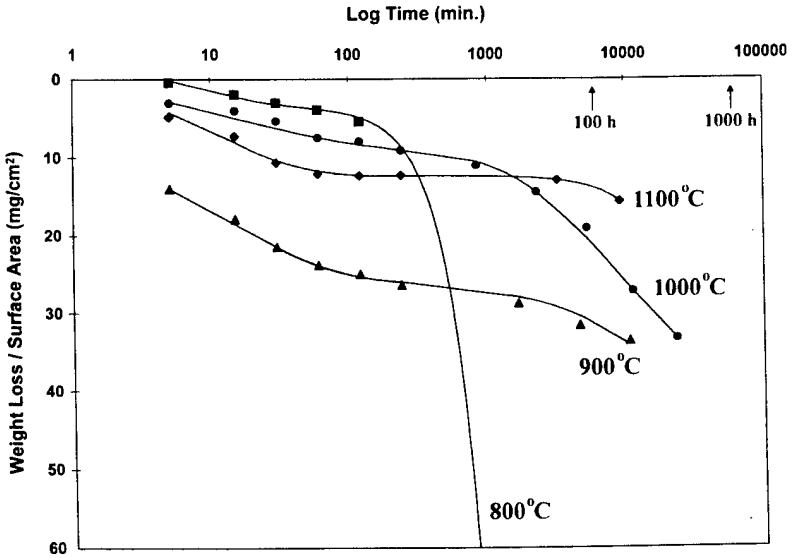

Figure 11. Wt. Loss/initial surface area vs. exposure time during cyclic oxidation in air of the homogenized, single-phase T2 Mo-12.5Si-25B alloy.

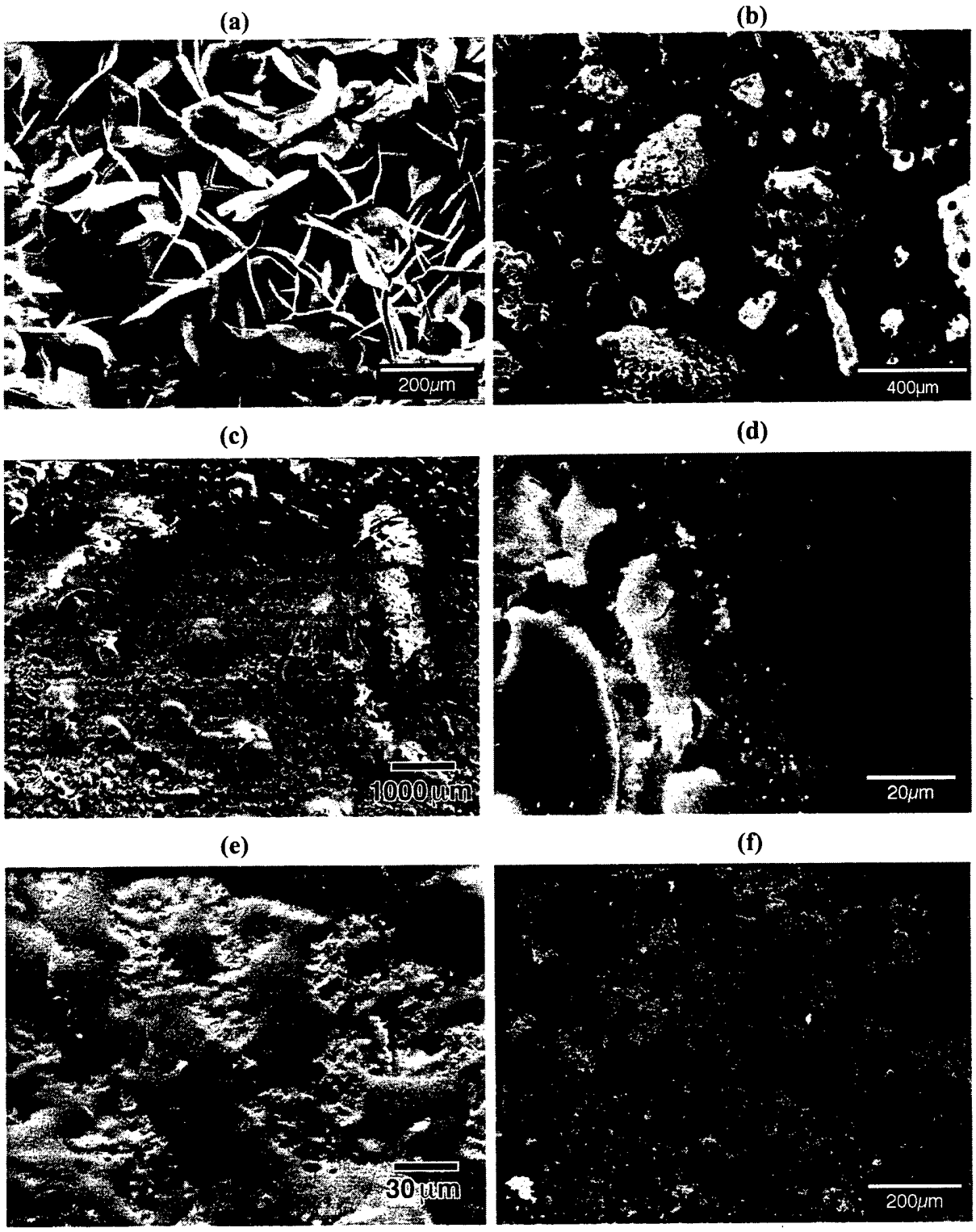

Figure 12. Microstructure of the oxide scale in the Mo-12.5Si-25B T2 alloy exposed to air at (a) 800°C, 15h, SEI; (b) 900°C, 15 mins., BEI; (c) 900°C, 98h, BEI; (d) 900°C, 178h, BEI; (e) 1000°C, 15 mins., BEI; and (f) 1000°C, 388h, BEI.

At 900 and 1000°C, the initial weight loss is higher, but becomes steadier at intermediate times to about 24h. This is followed by an apparent transition to higher weight losses at times beyond about 50h. The significant initial weight loss occurring at 900 and 1000°C in comparison with that at 800°C may be attributed to the increased reaction rates with temperature. The oxide scale at 900°C at initial to intermediate times appeared quite rough Figures 12(a,b), with many cracks and holes A glassy scale covered the samples at longer times, though protrusions and cracks were still present (Figure 12(d)). At 1000°C, the glassy scale formed at shorter times, though the surface was still rough and revealed protrusions and cracks (Figure 12(e)). At longer times, the glassy scale covered the sample surface, but Mo oxides were also present. As had been observed in the Mo1212 samples, MoO_3 and MoO_2 were detected in the scale of the samples tested at 900°C at short and longer times (Figures 13(a,b))). At 1000°C, both oxides were present at short times (Figure 14(a)), but at longer times only MoO_2 was present (Figure 14(b). These results indicate that the glassy scale is quite permeable to oxygen at 900°C, but becomes more viscous and less permeable to oxygen at 1000°C. The transition to near linear rates occurring at intermediate times at 900 and 1000°C may be the result of competing mechanisms for oxidation that occur due to changes in chemical composition of the scale during its growth that could influence the kinetics, or affect other properties such as viscosity or adhesion of the scale itself. At 900 and 1000°C in the Mo1225 samples at longer cyclic oxidation times, a degradation in properties occurs leading to a significant weight loss and failure of the materials. Lower, steady oxidation rates were observed at 1100°C, where a stable silica layer was formed.

Discussion

The results of this study have brought to light a number of important aspects relating to the oxidation behavior of Mo-Si-B alloys. These results are generally in good agreement with those of Mendiratta *et al.* [9,10], who reported on the cyclic oxidation behavior of the same three-phase Mo-12Si-12B alloy as in the present study at 750°C, 800°C, 1200°C and 1300°C.

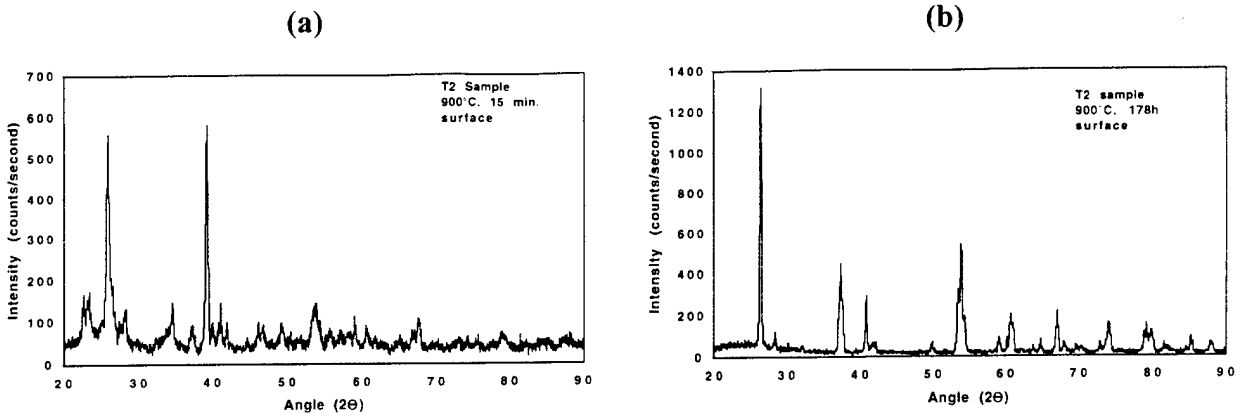

Figure 13. XRD patterns recorded from the surface of the oxide scale in the Mo-12.5Si-25B T2 alloy exposed to air at 900°C for (a) 15 mins and (b) 178h.

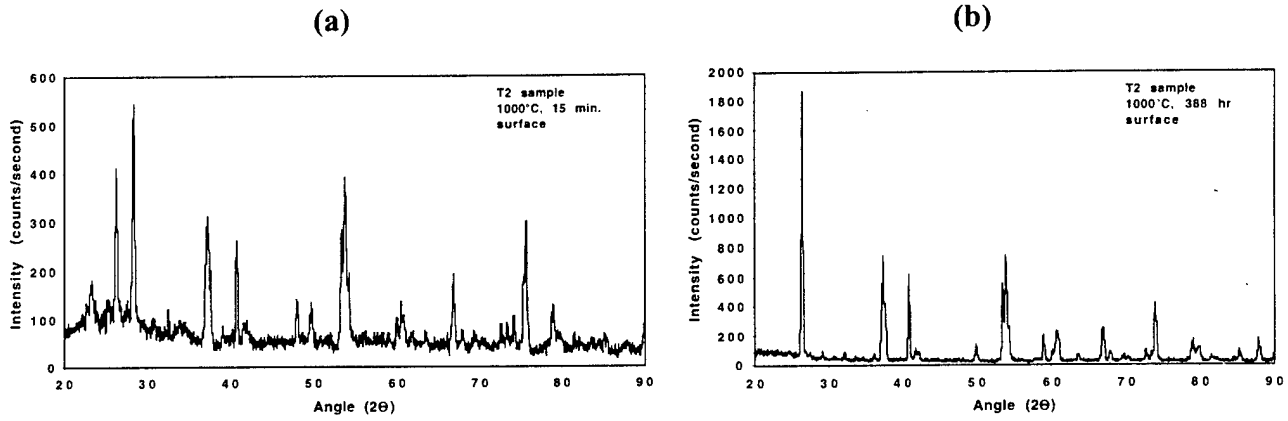

Figure 14. XRD patterns recorded from the surface of the oxide scale in the Mo-12.5Si-25B T2 alloy exposed to air at 1000°C for (a) 15 mins and (b) 388h.

In agreement with their findings [9], the present results on the cyclic oxidation kinetics and oxide scale microstructures indicate that there are two temperature regimes of behavior, the first from 900-800°C and lower and the second at 1000°C and higher. In these two regimes, there is competition between increasing weight loss due to volatilization of Mo as MoO_3 gas versus decreasing weight loss due to gradual formation of a stable, adherent silica layer, the former dominating in the lower temperature regime and the latter in the higher temperature regime. At both 800 and 900°C, a silica layer, presumably containing boron (i.e. a borosilicate), forms, but is quite fluid and porous (or permeable), owing to which diffusion of oxygen through the B-SiO_2

scale occurs easily, leading to continuous weight loss due to oxidation of Si and B and volatilization of Mo as MoO_3. The outer oxide scale contains spherical pores, which suggests that B may also be escaping as B_2O_3 gas; peaks corresponding to B_2O_3 could be seen in the XRD patterns, supporting this conclusion. However, sufficient B is presumably retained in the scale to make it both sufficiently fluid to cover the entire sample surface and permeable to oxygen, leading to rapid weight loss by escape Mo as MoO_3 gas. There is also evidence that B in SiO_2 significantly increases oxygen diffusivity [11]. At 1000°C, the weight loss in the transient period is similar to that at 900°C, due again to volatilization of Mo as MoO_3. However, the B-SiO_2 is formed more rapidly, covers the sample, is adherent, pore-free and begins to provide a measure of protection due to which the oxidation rates in the steady state are lower. However, the fact that weight is being lost continuously indicates that some MoO_3 gas is still escaping. In addition, boron from the B-SiO_2 scale may also be escaping, thereby progressively increasing the viscosity of the silica scale and providing both more resistance to oxygen diffusion and protection. Indeed, the fact that only MoO_2 and little or no MoO_3 is present supports this conclusion that oxygen diffusivity and partial pressure in the silica scale have been reduced. At 1100°C, the weight loss during the initial transient and in the steady state is lower. It appears that initial volatilizaiton of Mo as MoO_3 and B as B_2O_3 occurs very rapidly and leads to quick formation of a low B, high viscosity, adherent and protective silica scale,.

The oxidation behavior of the single-phase T2 Mo-12.5Si-25B alloy, in terms of operative mechanisms, is generally similar to that of the three-phase Mo-12Si-12B alloy. It appears, however, that the glassy B-SiO_2 scale does not form readily at 800°C, owing to which there is catastrophic weight loss by volatilization of Mo as MoO_3. At 900°C, the B-SiO_2 scale does form and provides some measure of protection. However, the coverage of this scale over the sample surface is not complete and also many cracks and pores are present, owing to which continuous weight loss occurs by volatilization of Mo as MoO_3. The extent of coverage of the B-SiO_2 scale is greater at 1000°C, which leads to lower oxidation rates to intermediate times. However, a transition of higher weight loss appears at longer times (>50h). This appears to be

related to the higher B content in the alloy, and hence, in the B-SiO_2 scale, which would render the scale more permeable to oxygen and allow continued formation and escape of MoO_3 gas, leading to weight loss. In effect, higher temperatures are required to remove the B in the B-SiO_2 scale as B_2O_3 gas and lower the viscosity and permeability of the scale to oxygen diffusion and provide stable protection. Thus, presumably this behavior occurs at 1100°C, leading to stable protection and reduced weight loss.

5. PERSONNEL SUPPORTED

The personnel supported in this project include Vijay K. Vasudevan (P.I.) and Keith J. Leonard (Postdoc, 50%).

6. NEW DISCOVERIES, INVENTIONS OR PATENT DISCLOSURES

The following are the major new findings resulting from this project.

- Thermal effects on microstructure evolution in a Mo-7.44Si-8.51B (at.%) alloy were studied:
  - The results indicate that it is possible to exert some control over microstructure and properties by very high temperature heat treatments
  - Significant changes in volume fraction of α-Mo, Mo_3Si and T2 phases occu at temperatures ≥1700°C
- The cyclic oxidation behavior in air at temperatures between 800-1100°C were studied in a three-phase Mo-12Si-12B (at.%) and near-single T2 phase Mo-12.5Si-25B alloy:
  - The results indicate that catastrophic oxidation occurs in both alloys at/below 800-900°C; performance and oxidation protection are better at ≥1000°C
  - A porous, non-protective borosilicate/B-SiO_2 layer forms at low temperatures, which permits easy oxygen diffusion and increased weight loss through volatilization of Mo as MoO_3 gas.
  - A stable, dense silica scale forms at/above 1000°C, which provides protection from oxidation and reduced weight loss

7. REFERENCES

1. D. M. Berczik, "Methods for Enhancing the Oxidation Resistance of a Molybdenum Alloy, and a Method of making an Molybdenum Alloy," *US Patent # 5595616*, January (1997).

2. D. M. Berczik, "Oxidation Resistant Molybdenum Alloy," *US Patent # 5693156* (1997).

3. M. K. Meyer and M. Akinc, *J. Amer. Cer. Soc.*, **79**, pp. 938-944 (1996).

4. M. K. Meyer, M. J. Kramer and M. Akinc, *Intermetallics*, **4**, pp. 273-281 (1996).

5. M. Akinc, M. K. Meyer, M. J. Kramer, A. J. Thom, J. J. Huebsch and B. Cook, *Mater. Sci. Engrg.*, **261**, 16 (1999).

6. M. K. Meyer, A. J. Thom and M. Akinc, *Intermetallics*, **7**, 153 (1999).

7. C. A. Nunes, R. Sakidja and J. H. Perepezko, *in: Structural Intermetallics*, M. V. Nathal *et al.* (eds.), TMS, Warrendale, PA, pp. 831-839 (1997).

8. J. H. Schneibel, C. T. Liu, D. S. Easton and C. A. Carmichael, *Mater. Sci. Engrg.*, **261A**, 78 (1999).

9. M. G. Mendiratta, T. A. Parthasarathy and D. M. Dimiduk, *Intermetallics*, **10**, pp. 225-232 (2002).

10. T. A. Parthasarathy, M. G. Mendiratta and D. M. Dimiduk, *Acta Mater.*, **50**, pp. 1857-1868 (2002).

11. N. P. Bansal and R. H. Doremus, in: *Handbook of Glass Properties*, Academic Press, Orlanod, FL (1986).

8. PRESENTATIONS

1. K. J. Leonard, B. Kowalski, M. G. Mendiratta and V. K. Vasudevan, "Microstructure and Oxidation Behavior of Mo-Si-B Intermetallic Alloys," *ASM Fall Meeting*," St. Louis, MO, October (2000).

2. K. J. Leonard, B. Mowalski and V. K. Vasudevan,"Microstructure Effects on Creep Behavior of Next generation of Refractory Alloys for Very High Temperature Applications," *AFOSR Metallic Materials Contractor's Meeting,* Monterey, CA (2000).

3. K. J. Leonard, B. Kowalski, M. G. Mendiratta and V. K. Vasudevan, "Oxidation Behavior of Mo-Si-B Intermetallic Alloys," *International Symposium on Structural and Functional Intermetallics*," Vancouver, BC, July (2000).

9. PUBLICATIONS

1. K. J. Leonard, B. Kowalski, M. G. Mendiratta and V. K. Vasudevan, "Microstructure and Oxidation Behavior of Mo-Si-B Intermetallic Alloys," *Intermetallics.*, in preparation.

2. K. J. Leonard, B. Kowalski, Q. Wu, M. G. Mendiratta and V. K. Vasudevan, "Oxidation Behavior of the Mo-12.5Si.25B (at.%) T2-Phase," *Scripta Mater.*, in preparation.

10. INTERACTIONS/TRANSITIONS

Several meetings have been held with Drs. Madan Mendiratta (UES) and Dennis Dimiduk (AFRL) to discuss project directions, priorities, materials and processing, areas of mutual interest, collaborations and courses of action. The Mo-Si-B materials investigated in this project were provided by Dr. Mendiratta and work on these materials was performed jointly. Joint presentations have resulted and joint journal articles are in preparation for submission.

11. HONORS/AWARDS

- *Neil Wandmacher Outstanding Teaching Award*, College of Engineering, University of Cincinnati (2000).
- *Fellow*, American Society for Materials International (2000).